Sustainable Food Technology

ROYAL SOCIETY OF CHEMISTRY

PAPER

View Article Online
View Journal | View Issue

Cite this: *Sustainable Food Technol.*, 2025, 3, 436

Encapsulation of fish oil in natural wax-based solid lipid particles using supercritical carbon dioxide: a green strategy to develop stable powder fish oil

Purlen Sezer Okur, [a] Deniz Ciftci[a] and Ozan N. Ciftci*[ab]

Fish oil has received significant attention owing to its high omega-3 fatty acid content. Regular fish oil consumption can supply enough omega-3 fatty acids to human metabolism. However, omega-3 fatty acids consist of a high amount of polyunsaturated fatty acids that are prone to oxidation, and hence, the storage, transportation, and processing of fish oil are challenging. Therefore, fish oil needs to be transformed into an easy-to-use and stable formulation. The objective of this study was to load fish oil into hollow solid lipid particles using a particle formation technique based on supercritical carbon dioxide (SC-CO_2). Powder formulations of fish oil were obtained using two different natural waxes, namely, candelilla and carnauba wax, at different initial fish oil concentrations (30, 40, and 50% w/w). All particles exhibited a spherical shape with a smooth surface. The melting point of the particles decreased on increasing the initial fish oil concentration. The highest loading efficiency was achieved at 50% w/w, with the initial fish oil concentration for candelilla and carnauba wax particles at 72.9% and 92.5%, respectively. Moreover, accelerated oxidative stability tests for 21 days of storage proved that the SC-CO_2-assisted particle formation technique successfully protected fish oil against oxidation and increased the shelf life of fish oil. Loading fish oil into waxes enhanced the bioaccessibility of EPA/DHA fatty acids regardless of the wax type, from 6.1% to 8.5% and 11.2% in CLW and CW particles, respectively. Thus, the findings suggest that SC-CO_2-assisted particle formation could be an efficient method for forming more stable fish oil formulations.

Received 17th November 2024
Accepted 21st December 2024

DOI: 10.1039/d4fb00345d

rsc.li/susfoodtech

Sustainability spotlight

Fish oil is a critical source of omega-3 fatty acids, which are essential for public health and disease prevention. However, its susceptibility to oxidation reduces its shelf life, diminishes its health benefits, and contributes to significant food loss and waste. Traditional encapsulation methods often require harmful organic solvents, which pollute the environment. In this study, we addressed these challenges by utilizing the supercritical CO_2 technology, a green and sustainable method, to encapsulate fish oil within natural waxes, creating a stable, free-flowing powder formulation. This innovative approach enhanced the oxidative stability, bioaccessibility, and shelf life of fish oil without using any harmful solvents. Aligning with the UN's multiple Sustainable Development Goals, it minimizes food waste, reduces environmental pollution, and provides a transportable, health-promoting ingredient suitable for food deserts, fighting malnutrition and lack of proper storage facilities, fostering sustainable food systems.

1 Introduction

Increasing consumption of health and wellness-promoting bioactive compounds has led to a rapid growth in the manufacturing of functional foods.[1] The consumption of health-beneficial long-chain polyunsaturated fatty acids (PUFAs), namely, eicosapentaenoic acid (EPA) and docosahexaenoic acid (DHA), is believed to have great health-promoting potential, especially for cardiovascular diseases.[2] The majority of findings prove that PUFAs could decrease the risk of type-2 diabetes and cardiovascular diseases if consumed in the recommended range of 250 to 1000 mg day^{-1}.[3] The human body cannot produce omega-3 fatty acids owing to the lack of desaturase enzymes.[4] Therefore, there is a growing interest in incorporating omega-3 oils into food formulations to develop health and wellness-promoting foods. However, incorporating omega-3 oils into foods is challenging owing to their low solubility, and also PUFAs are susceptible to oxidation owing to a high number of double bonds in their structure,[5] which results in degradation during either processing or storage. This degradation poses health risks to consumers and also causes food loss and waste, which are pressing issues of our era. Therefore, minimizing oxidation in food products is one way to overcome food loss and waste problems in lipid-rich foods.

[a]*Department of Food Science and Technology, University of Nebraska-Lincoln, Lincoln, NE, 68588-6205, USA. E-mail: ciftci@unl.edu*

[b]*Department of Biological Systems Engineering, University of Nebraska-Lincoln, Lincoln, NE, 68583-0726, USA*

Fish oil is a primary source of omega-3 fatty acids, yet its incorporation into food formulations encounters challenges. Owing to its water-insoluble nature, incorporating fish oil into water-based and solid foods is difficult, and its high polyunsaturated fatty acid (PUFA) content makes it highly susceptible to oxidation. Various encapsulation methods, such as spray drying, freeze drying, and electrohydrodynamic processes, have been proposed to reduce the oxidation rate and enhance shelf life.[5–7] Encapsulation serves several purposes, including protecting the encapsulated compounds from oxidative degradation, improving material handling, shielding contents from environmental stressors, and facilitating the incorporation of water-insoluble ingredients into food formulations. Ramos *et al.*[8] investigated the oxidative stability and encapsulation efficiency of fish oil using vacuum spray drying and conventional spray drying. Using maltodextrin and modified starch as wall materials, they demonstrated that vacuum spray drying, with its lower drying temperature, preserved fish oil better against oxidation compared to conventional spray drying. Another promising technique for fish oil encapsulation involves solid lipid nanoparticle technology, utilizing wall materials such as proteins, carbohydrates, or combinations of both.[9] The success of these processes often depends on the wall materials used and the intended application of the encapsulated product. For example, Salminen *et al.*[10] found that increasing the concentration of tristearin in encapsulates improved oxidative stability, emphasizing the importance of wall thickness in protecting fish oil.

An innovative approach for fish oil encapsulation is the supercritical carbon dioxide (SC-CO_2) technology.[11] SC-CO_2 is recognized as a generally safe (GRAS) solvent with several advantages: it is cost-effective, abundant, easily removed without leaving solvent residues, and operates at relatively low critical temperature and pressure values. SC-CO_2 assisted particle formation minimizes oxidation during encapsulation since oxygen is excluded from the particle formation environment, preventing oxidative degradation. In our previous studies, hollow solid lipid particles were developed using fully hydrogenated soybean oil (FHSO) as a wall material,[11] while Karim *et al.*[12] encapsulated fish oil with hydroxypropyl methylcellulose (HPMC) using a supercritical antisolvent technique. Additionally, polyethylene glycol was employed in the encapsulation of cod liver oil *via* the particles from the gas-saturated solution (PGSS) method.[13]

The SC-CO_2 technology and related particle formation techniques present valuable opportunities for protecting bioactive components like fish oil, enabling better oxidative stability, handling, and application versatility. However, the processing conditions and wall materials have a big impact on the properties of the products and their food applications. There is a need for detailed investigation of each wall material as they have different properties in the SC-CO_2 environment, which in turn affect the processing conditions and the product properties. In our previous studies, we used triacylglycerol-based solid lipids to load fish oil into solid lipids; however, there is a need for a more robust lipid shell to protect fish oil from oxidation completely.

Therefore, this study proposes using natural waxes—candelilla wax (CLW) and carnauba wax (CW)—as wall materials to create fish oil-loaded particles with a robust shell to enhance oxidative stability and extend shelf life. The project focuses on developing a natural, clean, and user-friendly powdered fish oil formulation without non-food-grade chemicals. Specifically, the project seeks to produce fish oil-loaded solid lipid particles from CLW and CW using SC-CO_2 technology. The objectives of this study are: (i) to examine how the initial fish oil concentration in the lipid blend affects the loading efficiency, particle morphology, particle size, melting properties, and polymorphic form; (ii) to assess the oxidative stability of fish oil-loaded solid wax particles; and (iii) to investigate the impact of the particle formation process on the bioaccessibility of EPA and DHA omega-3 fatty acids.

2 Materials and methods

2.1. Materials

Fish oil (26.7 mg total EPA-DHA/100 mg fish oil), candelilla wax (CLW), and carnauba wax (CW) were purchased from Sigma-Aldrich (St. Louis, MO, USA). Bone dry CO_2 (99.9% purity) was purchased from Matheson (Lincoln, NE).

2.2. Formation of fish oil-loaded micro- and nano-particles with SC-CO_2

Fish oil-loaded particles were formed by a homemade SC-CO_2 particle formation system reported previously.[14] The main steps for the particle formation remained the same. The vessel temperature was maintained at 65 and 85 °C for CLW and CW, respectively. Particles were formed at 100 bar using a 100 μm diameter nozzle based on the previously optimized conditions. To analyze the effect of the final concentration of fish oil in the lipid mixture, varying initial fish oil concentrations in the lipid mixtures (30, 40, and 50%, w/w) were used. The molten wax–fish oil mixture was placed into the vessel through the sampling port, and the lipid mixture was agitated in the presence of CO_2 for 1 h at 100 bar. Afterward, the SC-CO_2-expanded lipid mixture was atomized through the nozzle. The formed solid lipid particles were collected and kept at −20 °C until analyzed.

2.3. Determination of the particle size

The average particle size of the fish oil-loaded wax particles was analyzed using ImageJ software.[15] For each sample, three SEM images were captured with at least 100 particles from the same coordinates to calculate the average particle size of the sample. In total, the diameter of 300 particles was measured to calculate the average particle size for each sample.

2.4. Determination of the fish oil loading efficiency

Fish oil loading capacity was determined from the concentrations of EPA and DHA as distinctive fish oil fatty acids. Fish oil-loaded particles (~7 mg) and a physical mixture of fish oil and wax (control) at the corresponding concentrations (3 μL) were methylated, according to Yang & Ciftci.[16] Fatty acid methyl esters (FAME) were then analyzed using a gas chromatograph

(GC) (7890 GC systems, Agilent Technologies, Inc., Santa Clara, CA, USA) equipped with a flame ionization detector (FID). An aliquot of FAME (2 μL) was injected into an Agilent HP-INNOWAX capillary column (30 m × 0.25 mm × 0.25 μm) to separate the FAME. The GC oven temperature was held at 90 °C for 1 min, increased at a rate of 10 °C min^{-1} to 235 °C, and held at 235 °C for 5 min. Hydrogen was used as the carrier gas.

The concentrations of EPA and DHA were identified with authentic standards to determine the fish oil loading efficiency. Fish oil loading efficiencies (LE) of the particles were identified using eqn (1).

$$\text{LE}\ (\%) = \frac{\text{experimental loading capacity}}{\text{theoretical loading capacity}} \times 100 \quad (1)$$

Here, the experimental loading capacity is the total mass of EPA and DHA in the particle determined by GC, and the theoretical loading capacity is the total mass of EPA and DHA in the physical mixture of fish oil and wax.

2.5. Morphological analysis

2.5.1. Scanning electron microscopy (SEM) analysis. The morphology of the fish oil-loaded wax particles was analyzed by using a field-emission scanning electron microscope (S4700 FE-SEM, Hitachi High-Technologies Corporation, Tokyo, Japan) under a low vacuum mode at 5 kV and 15 mA. Sputtering of the samples was conducted in an argon atmosphere with chromium (Pfeiffer Vacuum, Aβlar, Germany).

2.5.2. Confocal fluorescence microscopy analysis. Fish oil loading into wax particles was visualized using a confocal fluorescence microscope (A1, Nikon Instruments Inc., Tokyo, Japan). Lipid particles were stained with Nile red solution (0.00125% w/v, in propane 1,2-diol).[16] To achieve adequate staining, 3–5 mg of particles were mixed with 100 μL of Nile red solution and stored at 4 °C overnight. Imaging was conducted with z-series scanning at 1 μm intervals. The excitation wavelengths were set to 561 nm and 640 nm, and the emission wavelength was fixed at 600 nm for the red fluorophores, enabling detailed visualization of the stained lipid particles.

2.6. Determination of polymorphism

Polymorphism of the fish oil-loaded wax particles, original wax, and hollow solid wax particles was analyzed using X-ray diffraction (XRD) with a PANanalytical system (Malvern, UK). Powder samples were measured at ambient temperature over a 2θ range from 2° to 50° using a continuous scan mode. The scanning parameters included a step size of 0.02° with a scan rate of 2θ min^{-1}.

2.7. Determination of melting behavior

The melting behavior of the original wax and fish oil-loaded wax particles was analyzed using a differential scanning calorimeter (DSC) (Netzsch DSC 204 F1 Phoenix, Netzsch, Germany). For each analysis, 3–5 mg of the sample was placed in an aluminum pan, with an empty pan serving as the reference. Both pans were equilibrated at 30 °C in the calorimeter for 1 min before starting the sequence. The samples were then heated from 30 °C to 100 °C at a controlled rate of 5 °C min^{-1}, allowing for precise measurement of melting transitions and thermal properties.

2.8. Oxidative stability

The oxidative stability of the fish oil-loaded wax particles was assessed *via* an accelerated oven test over a 21 day period. Both fish oil-loaded wax particles and pure fish oil were stored in open-lid containers at 40 °C in an oven to ensure the presence of excess oxygen. Oxidative stability was monitored daily by measuring the peroxide value, which indicates the formation of primary oxidation products, and the anisidine value, which reflects secondary oxidation products.

2.8.1. Peroxide value (PV). The peroxide value of the samples was determined using a modified colorimetric method based on Yang & Ciftci.[11] A chloroform/methanol mixture (7 : 3, v/v) was used to dilute the fish oil and fish oil-loaded wax particles (1–30 mg) to achieve a final absorbance of less than 1.0 cm^{-1}. In a test tube, 50 μL of the diluted sample was combined with 8 mL of chloroform/methanol (7 : 3, v/v). Subsequently, 50 μL each of ammonium thiocyanate and ferrous chloride solutions were added to the mixture. After vortexing for 10 s, the mixture was incubated for 20 min in a dark cabinet at room temperature. Following incubation, the absorbance was measured at 505 nm using a UV/Vis spectrophotometer (Evolution 201, Thermo Fisher Scientific, Shanghai, P. R. China). The hydroperoxide concentrations were determined against a cumene hydroperoxide standard curve (0–25 μM) and expressed as milliequivalents (meq.) of hydroperoxide per kg of fish oil.

2.8.2. Anisidine value (AV). The anisidine value (AV) of the fish oil-loaded particles and fish oil was determined following the AOCS Official Method Cd 18–90 with modifications.[17] Samples (1–30 mg, adjusted for secondary product concentration) were mixed with 8 mL of isooctane, and the absorbance (A_1) was measured at 350 nm using a UV/Vis spectrophotometer (Evolution 201, Thermo Fisher Scientific, Shanghai, P. R. China), with isooctane as the blank. Subsequently, 2.5 mL of the sample mixture or isooctane was transferred to a separate test tube, and 0.5 mL of *p*-anisidine solution (0.25% w/v in glacial acetic acid) was added. After vortexing for 10 s, the tubes were kept in a dark cabinet for 10 min at room temperature to complete the reaction. The absorbance (A_2) was then measured at 350 nm. The anisidine value was calculated using eqn (2):

$$\text{AV} = 8 \times \frac{1.2 \times A_2 - A_1}{\text{sample weight (g)}} \quad (2)$$

2.9. Simulated *in vitro* digestion

The simulated oral, gastric, and intestinal digestion approach, INFOGEST, was used to determine the *in vitro* bioaccessibility of omega-3 fatty acids, EPA and DHA in the crude fish oil and fish oil-loaded wax particles.[18] Simulated salivary fluid (SSF), simulated gastric fluid (SGF), and simulated intestinal fluid (SIF) were prepared using the corresponding electrolyte stock solutions according to Minekus *et al.*[18] All experiments were repeated five times.

2.9.1. Oral phase. The pre-heated (37 °C) SSF solution (8.95 mL) and the sample were mixed to obtain a uniform mixture of SSF and the sample. Then, 1 mL of α-amylase solution (750 U mL^{-1}) was added to achieve a 75 U mL^{-1} amylose unit. Next, 50 μL of 0.3 M $CaCl_2$ was added, and the pH of the mixture was adjusted to 7.0 using NaOH. The mixture was incubated at 37 °C for 2 min in a shaking water bath at 100 rpm.

2.9.2. Gastric phase. After the oral phase, 8.495 mL of SGF was mixed with an oral bolus (10 mL), and then the pH was adjusted to 3.0 using HCl. Then, 1 mL of porcine pepsin (40 000 U mL^{-1}), 0.5 mL of gastric lipase (1000 U mL^{-1}) and 5 μL of 0.3 M $CaCl_2$ were added to the mixture. The mixture was incubated at 37 °C for 2 h in a shaking water bath at 100 rpm.

2.9.3. Intestinal phase. After 2 h of gastric digestion, gastric chyme (20 mL) was mixed with 7.92 mL of SIF, and the pH was adjusted to 7.0 using NaOH. Next, 80 μL of 0.3 M $CaCl_2$, 4 mL of pancreatin (9 mg mL^{-1}), 4 mL of bile salt (130 mg mL^{-1}), and 4 mL of pancreatin lipase (80 mg mL^{-1}) were added to the mixture. Afterward, the final mixture (40 mL) was incubated at 37 °C for 2 h in a shaking water bath at 100 rpm.

2.9.4. Calculation of omega-3 bioaccessibility. After simulated digestion, 100 μL of Bowman–Birk inhibitor (0.05 g L^{-1}) per mL of the intestinal digest was added to the mixture to stop digestion. The entire solution was centrifuged at 10 000*g* for 45 min at 4 °C to collect the bioaccessible fraction. The bioaccessible fraction was filtered to separate the undigested oil from the aqueous phase. The filtered digested fluid was used to quantify the amount of omega-3 fatty acids. The oil in the filtered digested fluid was extracted using hexane (1 : 3; supernatant : hexane, v/v). The mixture of hexane and supernatant was vortexed for 10 min and centrifuged at 4400 rpm for 5 min at 4 °C to separate the hexane fraction. This procedure was repeated 3 times to obtain the oil in the aqueous phase. The hexane fraction was evaporated by flashing nitrogen. The fatty acid composition of extracts was analyzed using GC analysis, as described in section 2.4. Bioaccessibility of EPA + DHA was calculated using eqn (3) below.

$$\text{Bioaccessibility (\%)} = \frac{\text{EPA + DHA in the bioaccessible fraction}}{\text{total EPA + DHA in the sample}} \times 100 \quad (3)$$

2.10. Statistical analysis

All statistical analyses were performed using the SigmaPlot software package (SigmaPlot ver.14, Chicago, IL, USA). Data were analyzed through analysis of variance (ANOVA) and presented as mean ± standard deviation. Tukey's multiple range test was applied to compare the means and identify significant differences among factor levels, with a significance threshold set at $p \leq 0.05$.

3 Results and discussion

3.1. Fish oil loading efficiency

The fish oil loading efficiencies of CLW and CW particles are presented in Fig. 1. The highest loading efficiencies were achieved at a 50% (w/w) initial fish oil concentration in the lipid mixtures, reaching 73.9% and 92.5% for CLW and CW particles, respectively. The lowest loading efficiencies were found to be 42.9% for CLW and 43.1% for CW particles. A significant increase ($p \leq 0.05$) in loading efficiency was observed when the initial fish oil concentration increased from 30 to 50% (w/w).

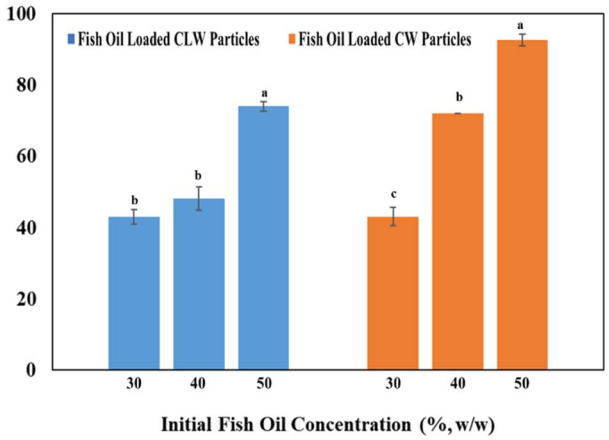

Fig. 1 Fish oil loading efficiency at different initial fish oil concentrations (%, w/w) for CLW and CW particles. Different letters represent significant differences among the loading efficiency values ($p \leq 0.05$).

The SC-CO_2-assisted particle formation process relies on the solubilization of CO_2 in the lipid phase and the volumetric expansion of the lipid mixture due to this solubilization. During the 1 h mixing time, SC-CO_2 and lipid phases equilibrated in the vessel, with the lipid volume constant at 20 mL. With constant CO_2 solubility at a fixed pressure and temperature, a higher initial fish oil concentration provided more liquid oil for encapsulation, resulting in significantly higher ($p \leq 0.05$) fish oil loading efficiencies in both CLW and CW particles. In our recent study on bioactive loading into triacylglycerol-based fats, namely, fully hydrogenated soybean oil (FHSO), increased lycopene concentration in the triacylglycerol mixture enhanced lycopene loading efficiency in FHSO particles, indicating that higher encapsulation efficiency is associated with greater availability of the lower melting point compound.[19]

However, the same initial fish oil concentration resulted in varying loading efficiencies between CLW and CW particles, with CW particles consistently showing higher loading efficiency. This difference was due to the higher solidification temperature of CW, which affects the cooling rate during particle solidification. Cooling rate impacts encapsulation efficiency, with CW's higher crystallinity supporting greater loading capacity.

3.2. Particle morphology

Fig. 2 presents the SEM images of the wax particles loaded with fish oil at varying initial fish oil concentrations and wax types. Across all samples, the particles maintained a spherical shape, but higher initial fish oil concentrations (from 30 to 50%, w/w) led to wrinkled surfaces in both candelilla (CLW) and carnauba wax (CW) particles. This wrinkling was due to the lower melting

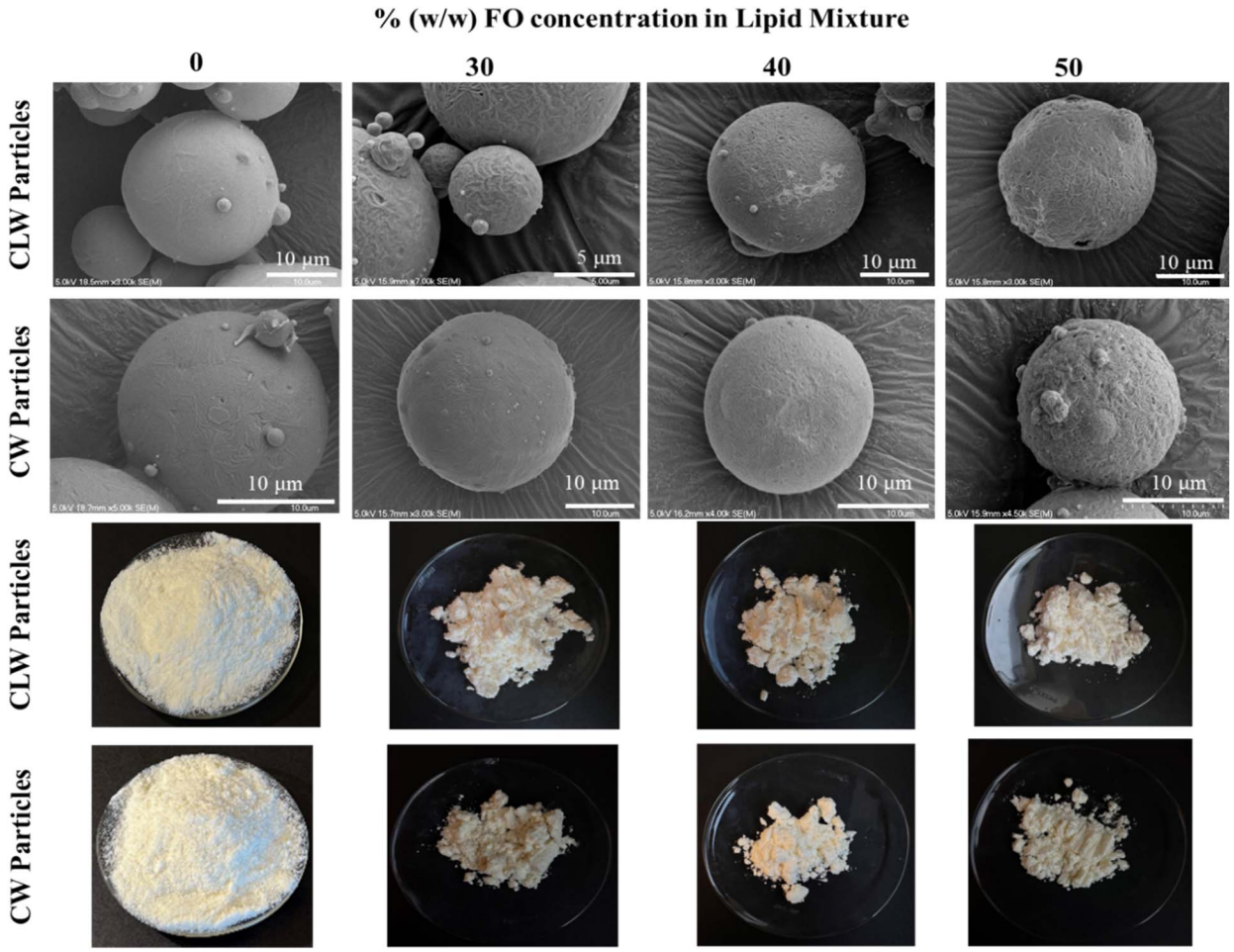

Fig. 2 SEM images (top) and the photographs (bottom) of the fish oil-loaded CLW and CW particles.

point of fish oil compared to CLW and CW, which influences the particle morphology. During rapid depressurization of the CO_2-expanded lipid mixture, the rapid cooling at the nozzle due to the Joule–Thompson effect causes the lipid blend droplets (fish oil + wax + CO_2) to solidify quickly. As the wax solidifies faster than fish oil, it traps the oil within, creating a wrinkled surface at higher fish oil concentrations.

To further assess the loading efficiency across fish oil concentrations, confocal fluorescence microscopy images were captured (Fig. 3). Hollow CW particles were used as controls. In the images, hollow areas appear black, while the fish oil (dyed with Nile red) is visible as pink. It is known that solid fat-dominated regions (CLW and CW) show low solubility of Nile red dye.[20] Results showed that particles with a 50% (w/w) initial fish oil concentration had more surface oil and internal fish oil. Additionally, smaller particles exhibited better loading efficiency, while larger particles contained less fish oil within their cavities, likely due to varying dye penetration depths across particle shells, with limited penetration leading to undyed cavities.[20]

3.3. Particle size analysis

The average sizes of particles with different initial fish oil concentrations are shown in Table 1. Results showed no significant difference in the average particle size by changing the fish oil concentration ($p > 0.05$). The average particle size of the fish oil-loaded particles ranged from 13.7 to 17.0 μm and

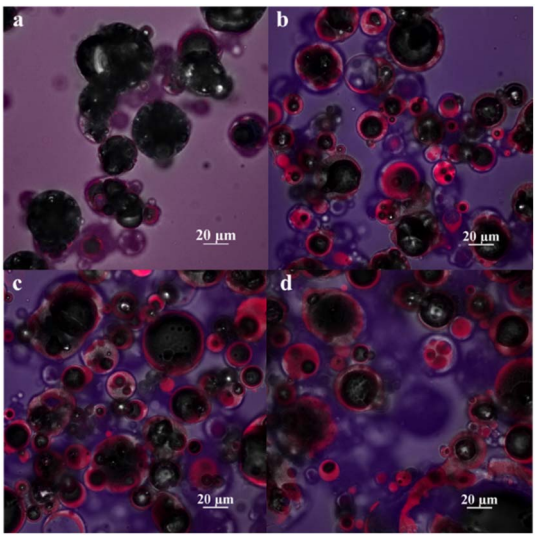

Fig. 3 Confocal microscopy images of the: (a) hollow CW particles, (b) 30%-CW, (c) 40%-CW, (d) 50%-CW.

Table 1 Average particle size of fish oil-loaded wax particles

Sample	Average particle size (μm)
30%-CLW	13.7 ± 0.6^a
40%-CLW	14.5 ± 1.3^a
50%-CLW	17.0 ± 2.9^a
30%-CW	12.9 ± 0.4^a
40%-CW	16.0 ± 0.3^a
50%-CW	16.3 ± 0.7^a

[a] Means with different letters are significantly different ($p \leq 0.05$).

12.9 to 16.3 μm for CLW and CW, respectively. It was found that increasing the initial fish oil concentration resulted in larger particles. These data were also in good agreement with the visual observations from the SEM images.

The disadvantage of the higher initial fish oil concentration was the agglomeration of particles. With increasing surface oil on the particles and increasing initial fish oil concentration, the liquid oil on the surface of the particles caused the particles to stick to each other, causing agglomeration. However, this effect was not significant because the particles were in the powder form at all conditions. Previously, it was reported that even though particles agglomerate, they remain in the powder form.[21]

3.4. Polymorphism

One of the important parameters that affect the melting properties and release of the loaded materials from the solid lipid particles is the polymorphic form of the particles. The crystal type of the lipid forming the solid shell is related to the release kinetics and stability of the loaded material in lipid carrier systems.[22] Crystal types of fats could be α, β′, and β in the increasing order of melting point, packing density, and thermodynamic stability. Fig. 4 shows that particle formation did not affect the major polymorphic form of the hollow solid lipid particles and fish oil-loaded particles. XRD patterns of the fish oil-loaded particles prove that loading fish oil into particles and increasing the initial fish oil content did not affect the major polymorphic form.

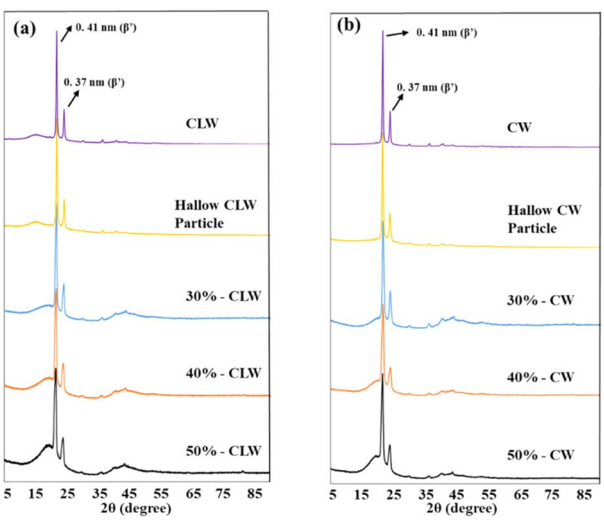

Fig. 4 XRD patterns of fish oil-loaded CLW (a) and CW (b) particles.

All samples showed peaks at 21.4 and 23.9°, which represented the stable β′ type of crystals with short spacings of 4.1 and 3.7 Å.[23] The diffraction patterns of wax, hollow solid wax particles, and fish oil-loaded wax particles exhibited the same peaks as β′, which is related to the polymorphism of pure wax. β′ type of crystals with short spacings of 4.1 and 3.7 Å indicate the particles were partially crystalline, and these spacings are characteristic of the orthorhombic subcellular packing in lipids. These results show that the lipid material used as the carrier matrix affects the polymorphism of the particles, which is critical for real-life applications. Our previous study with triacylglycerol-based fats has shown that the polymorphism of the particle changes after the particle formation process. The polymorphic form of the fully hydrogenated soybean oil changed from the more stable forms of β′ and β to a less stable form of α. These new findings show that the lipid shell composition and the solidification rate during SC-CO_2-assisted atomization, a function of the lipid composition, are critical for the polymorphic forms of the particles and determine their physical stability during storage and potential applications in the food industry.

3.5. Melting behavior

Differential scanning calorimetry (DSC) thermograms for the heating phase of hollow particles and fish oil-loaded particles with varying initial fish oil concentrations are presented in Fig. 5a and b. Analysis of the melting behavior confirmed that the melting temperature of the particles decreased as the initial fish oil concentration in the lipid matrix increased. This decrease aligns with expectations, as the fish oil—having a lower melting point than pure wax due to higher amounts of unsaturated fatty acids—lowers the overall melting temperature of the lipid blend. Notably, the melting profile, characterized by a single sharp peak at the melting point, remained consistent across samples, indicating uniform melting behavior. The polymorphic form of the lipid significantly influences the melting properties of the particles. In this study, all samples displayed the β′ polymorphic form, suggesting that the observed single melting peak corresponds to a single crystal type. The melting temperatures ranged from 67.7 to 60.1 °C for CLW particles and from 86 °C to 82.4 °C for CW particles, as the initial fish oil concentration increased from 0 to 50% w/w. This shift in melting point is attributed to the addition of fish oil, which has a lower melting point, to the lipid blend because there was no change in the polymorphic form of the particles. Moreover, while the melting peak shifted downward with the higher liquid oil content in the particle formation blend, the peak shape remained similar across concentrations.

3.6. Oxidative stability

To evaluate the oxidative stability of the particles, peroxide value (PV) and anisidine value (AV) were measured for 21 days of

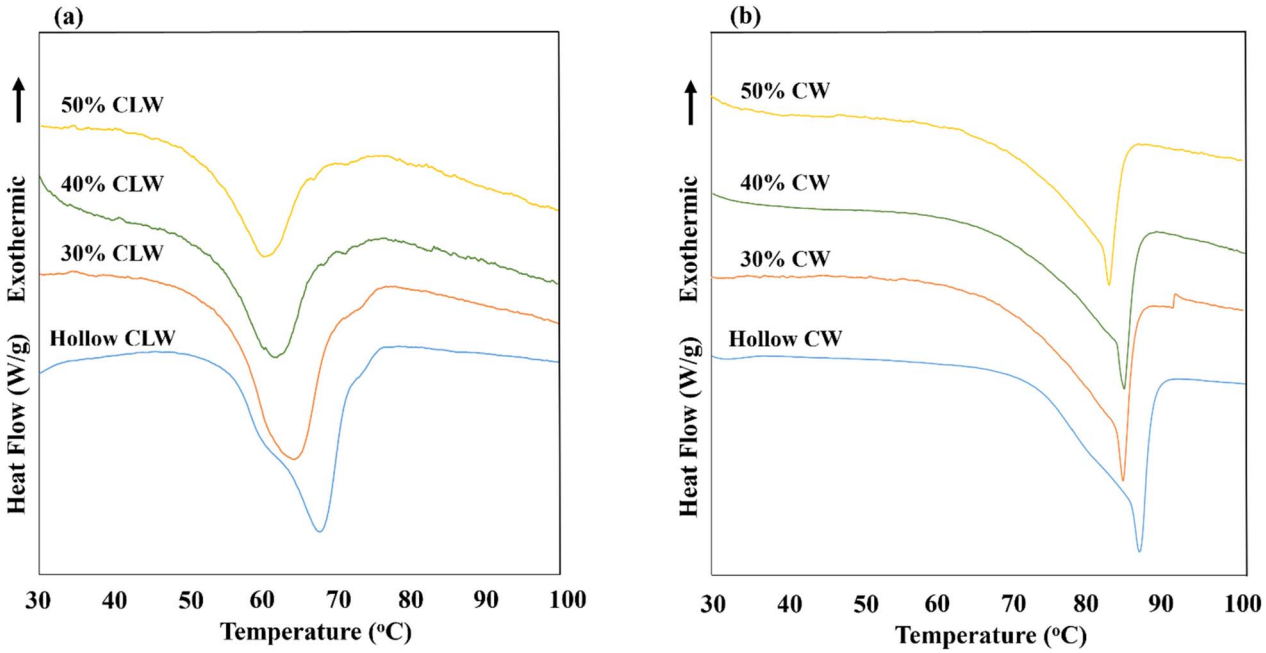

Fig. 5 Melting behavior of fish oil-loaded CLW particles (a) and CW particles (b).

storage period at 40 °C, with fish oil as the control. The results for primary oxidation products are presented in Fig. 6a, while secondary oxidation products are shown in Fig. 6b.

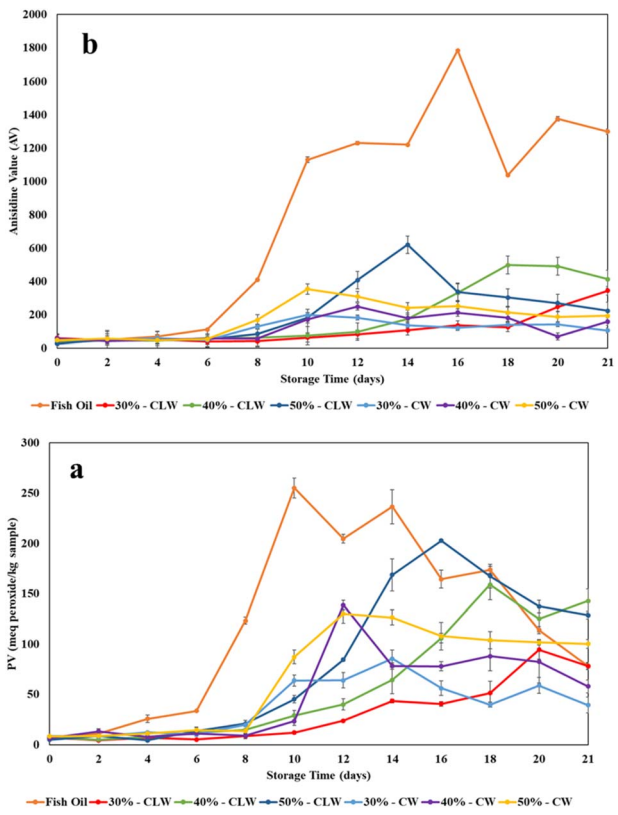

Fig. 6 (a) Peroxide value (PV) and (b) anisidine value (AV) of the fish oil and fish oil-loaded wax particles during three weeks of storage at 40 °C.

Encapsulating fish oil in hollow wax particles was employed as a strategy to protect polyunsaturated fatty acids (PUFAs) from oxidative degradation. The study found that particle formation using supercritical CO_2 (SC-CO_2) significantly improved the oxidative stability of fish oil, as indicated by both primary and secondary oxidation metrics. Additionally, the PV and AV values measured immediately after particle formation (day 0) suggested that the SC-CO_2-assisted particle formation did not cause oxidation, even under high-temperature conditions, contrasting with the effects seen in spray drying processes. El-Messery *et al.*[24] previously reported that spray-dried fish oil particles exhibited higher PV values due to the elevated process temperatures required. In the SC-CO_2 process, the absence of oxygen in the CO_2 environment eliminates oxidation even at high temperatures, offering a distinct advantage over spray drying by protecting heat-sensitive compounds, such as polyunsaturated (PUFA) oils like fish oil, from degradation, making it a promising technology for the processing of fish oil and similar PUFA oils. For all samples, including those with varying initial fish oil concentrations and types of wax, an increase in PV and AV values was observed after 6 days, similar to free fish oil. However, the rate of oxidation was slower in fish oil-loaded particles compared to free fish oil. While free fish oil showed a sharp increase in oxidation rate after day 6, encapsulated fish oil exhibited a more gradual increase, demonstrating that encapsulation effectively mitigated oxidation. These results were in agreement with a previous study that identified the effect of the solid lipid concentration in the particle formation mixture.[20] It was found that increasing solid lipid concentration can result in better protection against oxidation. Furthermore, fish oil-loaded particles with identical oil concentrations but different wax types showed varying oxidative stability during the storage period. Specifically, CW particles demonstrated

superior oxidative stability compared to CLW particles, likely due to the higher melting point of CW, which may reduce oxygen permeation into the cavity of the particles and thereby enhance stability.

3.7. *In vitro* bioaccessibility of omega-3 fatty acids

This study investigated the effect of the wall material—specifically, candelilla wax (CLW) and carnauba wax (CW)—on the bioaccessibility of omega-3 fatty acids in powdered fish oil formulations. Fish oil-loaded wax particles with the highest loading efficiency were selected to analyze the EPA and DHA bioaccessibility (Fig. 7). Bioaccessibility measurement is crucial, as it reflects the transfer capability of loaded compounds from the particles to mixed micelles during digestion.[25] The bioaccessibility of EPA/DHA in crude fish oil was found to be 6.1%, which increased to 8.5 and 11.2% in CLW and CW particles, respectively. These results indicate that the SC-CO_2-assisted particle formation process can enhance omega-3 bioaccessibility. Both CLW and CW were utilized as wall materials to form fish oil-loaded lipid particles, and as non-digestible lipids, they enable two potential mechanisms for micellar bioaccessibility during digestion:[26] the loaded material may either transfer by simple diffusion or be solubilized by simple micelles composed of bile salts and phospholipids. The findings showed that, despite the non-digestibility of the wall materials used in this study, the bioaccessibility of EPA and DHA increased after particle formation. Additionally, the bioaccessibility of EPA and DHA was higher when CW was used as the wall material. The wax composition of CLW and CW differs significantly; CLW is primarily composed of hydrocarbons, while CW consists of over 80% wax esters.[7] A higher melting point wax forms a harder particle shell, which provides superior encapsulation and protection of bioactive components during digestion. Consequently, encapsulation with CLW and CW improved the stability of fish oil, allowing EPA and DHA fatty acids to transfer into the micellar phase during the intestinal digestion stage.

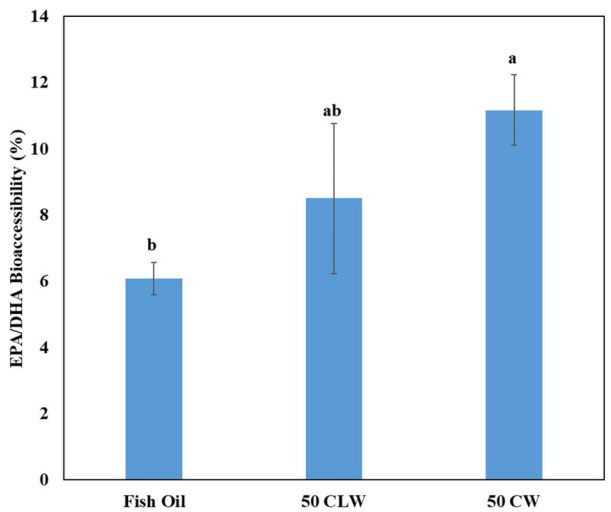

Fig. 7 EPA/DHA bioaccessibility (%) after simulated digestion. Different letters represent significant differences among the bioaccessibility values of EPA/DHA ($p \leq 0.05$).

4. Conclusions

Due to the susceptibility of fish oil to oxidation, which complicates its utilization, transportation, and storage, encapsulation is a promising strategy to inhibit the oxidation of its health-promoting components. In this study, a powdered fish oil formulation was successfully developed using two natural waxes as encapsulating wall materials. The SC-CO_2-assisted particle formation process emerged as an effective approach for fish oil encapsulation, with natural waxes—candelilla wax (CLW) and carnauba wax (CW)—significantly enhancing oxidative stability. The formation of primary oxidation products was delayed during the period from 6 days to 10–12 days, affecting the stability of particles. The improved oxidative stability observed in these hollow solid lipid particles indicates that particle shell thickness is tunable, with natural waxes offering an excellent option for creating a robust shell. Additionally, encapsulating fish oil with natural waxes increased the oxidative stability of omega-3 fatty acids, specifically EPA and DHA, further supporting the effectiveness of this encapsulation method. Particle formation using natural waxes not only protected omega-3 fatty acids against oxidation but also improved the bioaccessibility of omega-3 fatty acids from 6.1 to 11.2% by loading into CW particles. Nonetheless, further investigations will be conducted to evaluate the performance of the particles in real food systems and their overall quality in the foods.

Data availability

Data are available from the authors upon request.

Author contributions

Purlen Sezer Okur: investigation, data curation, formal analysis, writing – original draft preparation, writing – reviewing and editing; Deniz Ciftci: methodology, formal analysis, funding acquisition, writing – reviewing and editing; Ozan Ciftci: conceptualization, supervision, project administration, funding acquisition, resources, writing – reviewing and editing.

Conflicts of interest

Ozan Ciftci, author of this study, has disclosed a significant financial interest in Cargill, Inc. In accordance with its Conflict of Interest policy, the University of Nebraska-Lincoln's Conflict of Interest in Research Committee has determined that this must be disclosed.

Acknowledgements

This project is funded by the USDA NIFA Novel Foods and Innovative Manufacturing Technologies program (Awards #: 2021-67017-33342). Part of the research was performed in the Nebraska Nanoscale Facility: National Nanotechnology Coordinated Infrastructure and the Nebraska Center for Materials and Nanoscience (and/or NERFC), which are supported by the National Science Foundation under Award ECCS: 2025298, and

the Nebraska Research Initiative. The authors also thank the Morison Microscopy Core Research Facility for SEM and confocal microscopy.

References

1 E. J. Baker, *Curr. Opin. Clin. Nutr. Metab. Care*, 2024, **27**, 106–115.
2 N. Rubio-Rodríguez, S. M. de Diego, S. Beltrán, I. Jaime, M. T. Sanz and J. Rovira, *J. Supercrit. Fluids*, 2008, **47**, 215–226.
3 S. A. Strobel, K. Hudnall, B. Arbaugh, J. C. Cunniffe, H. B. Scher and T. Jeoh, *Food Bioprocess Technol.*, 2019, **13**, 275–287.
4 M. E. Surette, *CMAJ*, 2008, **178**, 177–180.
5 M. Aghbashlo, H. Mobli, A. Madadlou and S. Rafiee, *Food Bioprocess Technol.*, 2012, **6**, 1561–1569.
6 M. Jiang, Z. Hu, Y. Huang, X. D. Chen and P. Wu, *Food Res. Int.*, 2024, **191**, 114646.
7 Y. Soleimanian, S. A. H. Goli, A. Shirvani, A. Elmizadeh and A. G. Marangoni, *Compr. Rev. Food Sci. Food Saf.*, 2020, **19**, 2994–3030.
8 F. M. Ramos, V. Silveira Junior and A. S. Prata, *Food Res. Int.*, 2021, **143**, 110283.
9 S. Khoshnoudi-Nia, Z. Forghani and S. M. Jafari, *Crit. Rev. Food Sci. Nutr.*, 2022, **62**, 2061–2082.
10 H. Salminen, T. Helgason, B. Kristinsson, K. Kristbergsson and J. Weiss, *J. Colloid Interface Sci.*, 2017, **490**, 207–216.
11 J. Yang and O. N. Ciftci, *Food Chem.*, 2017, **231**, 105–113.
12 F. T. Karim, K. Ghafoor, S. Ferdosh, F. Al-Juhaimi, E. Ali, K. B. Yunus, M. H. Hamed, A. Islam, M. Asif and M. Z. I. Sarker, *J. Food Drug Anal.*, 2017, **25**, 654–666.
13 S.-C. Lee, D. Surendhiran and B.-S. Chun, *J. CO2 Util.*, 2022, **62**, 102104.
14 J. Yang and O. N. Ciftci, *Food Bioprod. Process.*, 2016, **98**, 151–160.
15 A. Ubeyitogullari and O. N. Ciftci, *J. Food Eng.*, 2017, **207**, 99–107.
16 J. Yang and O. N. Ciftci, *Food Funct.*, 2020, **11**, 8637–8647.
17 F. D. AOCS, *AOCS*, 1998, **5**, 2–93.
18 M. Minekus, M. Alminger, P. Alvito, S. Ballance, T. Bohn, C. Bourlieu, F. Carriere, R. Boutrou, M. Corredig, D. Dupont, C. Dufour, L. Egger, M. Golding, S. Karakaya, B. Kirkhus, S. Le Feunteun, U. Lesmes, A. Macierzanka, A. Mackie, S. Marze, D. J. McClements, O. Menard, I. Recio, C. N. Santos, R. P. Singh, G. E. Vegarud, M. S. Wickham, W. Weitschies and A. Brodkorb, *Food Funct.*, 2014, **5**, 1113–1124.
19 P. Sezer Okur and O. N. Ciftci, *Food Bioprocess Technol.*, 2024, **17**(7), 2048–2060.
20 S. Davis, J. Haldipur, Y. Zhao, N. Dan, Y. Pan, N. Nitin and R. V. Tikekar, *LWT–Food Sci. Technol.*, 2015, **64**, 14–17.
21 R. V. Tikekar and N. Nitin, *Langmuir*, 2012, **28**, 9233–9243.
22 A. Linke, J. Hinrichs and R. Kohlus, *Powder Technol.*, 2020, **364**, 115–122.
23 C. Liu, Z. Zheng, Z. Meng, X. Chai, C. Cao and Y. Liu, *LWT–Food Sci. Technol.*, 2019, 115.
24 T. M. El-Messery, U. Altuntas, G. Altin and B. Özçelik, *Food Hydrocolloids*, 2020, 106.
25 V. da Silva Santos, A. P. Badan Ribeiro and M. H. Andrade Santana, *Food Res. Int.*, 2019, **122**, 610–626.
26 D. J. McClements, *Food Funct.*, 2018, **9**, 22–41.